

Pulsar timing array results sheds light on Hubble tension during the end of inflation

M. Bousder^{1*}, E. Salmani^{1,2}, A.Riadsolh³,
H. Ez-Zahraouy^{1,2}, A. El Fatimy^{4,5} and M. El Belkacemi³

¹Laboratory of Condensend Matter and Interdisciplinary Sciences, Department of physics,
Faculty of Sciences, Mohammed V University in Rabat, Morocco

²CNRST Labeled Research Unit (URL-CNRST), Morocco

³Laboratory of Conception and Systems (Electronics, Signals and Informatics)
Faculty of Sciences, Mohammed V University in Rabat, Morocco

⁴Central European Institute od Technology,
CEITEC BUT, Purkyňova 656/123, 61200 Brno, Czech Republic

⁵Departement of Physics, Université Mohammed VI Polytechnique, Ben Guerir 43150, Morocco

November 8, 2023

Abstract

Recently, pulsar timing array (PTA) collaborations, including NANOGrav, have reported evidence of a stochastic gravitational wave background within the nHz frequency range. It can be interpreted by gravitational waves from preheating era. In this context, we demonstrate that the emission of this stochastic gravitational wave background can be attributed to fluctuations occurring at the end of inflation, thus giving rise to the Hubble tension issue. At the onset of inflation, the value of the frequency of the gravitational wave signal stood at $f = 0.08nHz$, but it rapidly transitioned to $f = 1nHz$ precisely at the end of inflation. However, just before the end of inflation, a phase characterized by curvature perturbation is known to occur, causing a swift increase in the frequency.

Keywords: Pulsar timing array, gravitational wave, inflation, Hubble tension.

*mostafa.bousder@fsr.um5.ac.ma

1 Introduction

The stochastic gravitational wave (GW) signals at nHz frequencies in the 15-year data set [1, 2] and 12.5-year data [3, 4], has recently garnered significant attention. This data has been published by the North American Nanohertz Observatory for Gravitational Waves (NANOGrav) collaboration. The GW signal may arise following the power-law distribution of abundance: $\Omega_{GW} \propto f^\zeta$. NANOGrav's observations indicate that the exponent ζ lies within the range of $(-1.5, 0.5)$ at a frequency of $f = 5.5nHz$. In response to the NANOGrav results, a series of recent gravitational wave models, [5, 6, 7], have been proposed. Often the authors linked this signal with cosmic inflation [8, 9] and from axion inflation [10]. This signal has the potential to be construed as an outcome of the stochastic gravitational wave background emanating from primordial black holes (PBHs) formed during inflation, [11, 12, 13, 14, 15, 16]. Conversely, alternative studies propose that cosmic strings might serve as the origin of these waves, as indicated in [17].

The authors in [18] explore gravitational wave production during the end of inflation (preheating). This process generates significant inhomogeneities, leading to a stochastic background of gravitational waves within the comoving Hubble horizon at the end of inflation. Importantly, their results emphasize that the current amplitude of these gravitational waves is independent of the inflationary energy scale. The analysis focuses on a specific model with an inflationary energy scale of approximately $10^9 GeV$. This discovery highlights the potential for a new observational perspective on inflationary physics and encourages further investigations into stochastic gravitational wave backgrounds across the Hz to GHz frequency range, characterized by an amplitude of $\Omega_{GW} h^2 \sim 10^{-11}$. Moreover, their computational approach has broader applications for understanding gravitational waves originating from various inhomogeneous processes in the early universe. The paper [19] considers a scenario in which the end of inflation is treated as a sudden event, and it provides mathematical formulations for essential parameters such as the spectrum, spectral tilt, and non-Gaussianity. These formulas are then applied to analyze a minimal extension of the initial hybrid inflation model, shedding light on the intricate dynamics of the early universe.

The Measurements of the current rate of expansion of the Universe conducted on a local scale, utilizing observations of Type Ia Supernovae (SNeIa) through the Hubble Space Telescope (HST), exhibit values that tend to cluster around $H_0 \simeq (73.24 \pm 1.74) km.s^{-1}.Mpc^{-1}$ [20]. In contrast, calculations of the Hubble constant derived from measurements of the Cosmic Microwave Background (CMB) indicate a value of approximately $H_0 \simeq (67.27 \pm 0.66) km.s^{-1}.Mpc^{-1}$ [21]. This introduces a deviation of 4σ or more from the local measurements. One of the more effective resolutions to the Hubble tension

[22, 23, 24, 25, 26] involves incorporating an early dark energy component [27] or introducing primordial magnetic fields [28]. Additionally, numerous studies have approached this issue by imposing constraints.

The purpose of the present paper is to introduce an interpretation of the Hubble tension from NANOGrav signal at the end of inflation.

This paper is organized as follows. In Sec. 2, we review the stochastic gravitational wave background from the tensor perturbation and the gravitational wave spectrum. In Sec. 3, we analyze the Hubble tension in inflationary epoch. In Sec. 4, the e-folding number, slow roll parameter and spectral index are studied. In Sec. 5, we study the energy density spectrum in the end of inflation. We conclude our findings in Sec. 6.

2 Amplitude of the GW signal

The action of the gravitational wave sources represented by the tensor perturbation h_{ij} ($i, j = 1, 2, 3$) is

$$S = \int d\tau d^3x \sqrt{-\delta} \left[\frac{-\delta^{\mu\nu}}{64\pi G} \partial_\mu h_{ij} \partial_\nu h^{ij} + \frac{1}{2} \Pi_{ij} h^{ij} \right], \quad (2.1)$$

where G is the Newtonian gravitational constant, τ is the conformal time and Π_{ij} corresponds to an anisotropic stress, encompassing the impact of a macroscopic magnetic field. Here $\delta_{\mu\nu}$ in the Minkowski metric of flat spacetime [29] $g_{\mu\nu} = \delta_{\mu\nu} + h_{\mu\nu}$ ($\mu, \nu = 0, 1, 2, 3$). The Friedmann-Robertson-Walker (FRW) spacetime [30]:

$$ds^2 = (ic^2 dt)^2 - a^2(t) (\delta_{ij} + h_{ij}) dx^i dx^j, \quad (2.2)$$

where $a(t)$ is the scale factor with $ad\tau = dt$. The Hubble parameter is defined as $H = \dot{a}/a$ where \dot{a} signifies the derivative of a with respect to time. we write the conditions on the tensor h_{ij} as $\partial^i h_{ij} = h^i_i = 0$.

We can perform a Fourier transformation of the gravitational wave field by [31, 32, 33]:

$$h_{ij}(\tau, \vec{x}) = \int \frac{d^3\vec{k}}{(2\pi)^{3/2}} \sum_{s=+, \times} \left[h_k(\tau) \epsilon_{ij} C(\vec{k}) e^{i\vec{k}\vec{x}} + cc \right], \quad (2.3)$$

where $k = |\vec{k}| = 2\pi f$ is the GW wavenumber and cc stands for the complex conjugate term. Here, the ϵ_{ij} satisfy the conditions $\delta^{ij} \epsilon_{ij} = 0$. The energy density of the gravitational waves is expressed as follows [30]:

$$\rho_{GW} = \frac{1}{64\pi G} \left\langle (\partial_t h_{ij})^2 + \frac{1}{a^2} (\nabla h_{ij})^2 \right\rangle, \quad (2.4)$$

where the bracket $\langle \bullet \rangle$ describes the spatial average. To describe the spectral amplitude of GWs, we employ the dimensionless parameter $\Omega_{GW} = \rho_{GW}/\rho_{crit}$ where $\rho_{crit} = \frac{3H_0^2}{8\pi G}$.

This parameter signifies the energy density of GWs within each logarithmic frequency interval:

$$\Omega_{GW}(f) = \frac{1}{\rho_{crit}} \frac{d\rho_{GW}}{d \ln f}, \quad (2.5)$$

where H_0 is the current Hubble constant and f is the frequency of the GW signal. An approximation for the gravitational wave spectrum can be made by employing the power-law model:

$$\Omega_{GW}(f) = \Omega_{GW*} \left(\frac{f}{f_*} \right)^{n_s(f)}, \quad (2.6)$$

where $\Omega_{GW*} = \Omega_{GW}(f = f_*)$. The spectral index is

$$n_s(f) = \begin{cases} n_{GW1} & \text{for } f < f_* \\ n_{GW2} & \text{for } f > f_* \end{cases}. \quad (2.7)$$

We notice that for $f = f_*$, we get $n_{GW1} = n_{GW2}$. If $n_s = -1$, we obtain $f\Omega_{GW} = f_*\Omega_{GW*}$.

3 Hubble tension from GW signal

Hubble tension from GW signal [34, 13]. The current amplitude of the gravitational wave signal observed today is given by [35, 36]

$$\Omega_{GW}(f) = \frac{\Omega_{R,0}}{24} \mathcal{P}_h(f), \quad (3.1)$$

where $\Omega_{R,0} \approx 8.6 \times 10^{-5}$ is the radiation energy density today and $\mathcal{P}_h(f)$ is the power spectrum of tensor fluctuations, which varies with frequency, at the moment of exiting the cosmic horizon. We can establish a connection between the e-folding number N and the GW frequency of the signal f , such that [35]:

$$N = N_{CMB} + \ln \frac{k_{CMB}}{0.002 Mpc^{-1}} - 44.9 - \ln \frac{f}{10^2 Hz}. \quad (3.2)$$

We notice that $N = 0$ at the end of inflation. While, in the CMB scale we have $k_{CMB} = 0.002 Mpc^{-1}$ and $N_{CMB} \sim 50 - 60$, in this case we get

$$N = N_{CMB} - 44.9 - \ln \frac{f}{10^2 Hz}. \quad (3.3)$$

Or equivalently

$$N = \ln \frac{10^2 e^{N_{CMB} - 44.9} Hz}{f}. \quad (3.4)$$

Thus, the e-folding number can be expressed as

$$N = \ln \frac{f_*}{f}, \quad (3.5)$$

where $f_* = 10^2 e^{(N_{CMB}-44.9)} Hz$ is the typical frequency. Based on this relation, it's noteworthy that the state represented by $f_* = f$ describes the end of inflation. Conversely, in order to align the value of N with observational data, we need to take into account the following condition:

$$f < f_*. \quad (3.6)$$

This condition is comparable with $n_s = n_{GW1}$ (2.7). On the other hand, the equations (2.6) and (3.5) take this form,

$$\Omega_{GW}(f) = \Omega_{GW*} e^{n_s(f)N}. \quad (3.7)$$

At the end of inflation, we find $\Omega_{GW}(f) \approx \Omega_{GW*}$. The Planck CMB data implies that $n_s \approx 0.965 \pm 0.004$ [21]. It is easy to see from $N_{CMB} \sim 50$ that

$$\Omega_{GW}(f) = \Omega_{GW*} e^{48.25 \pm 0.2}. \quad (3.8)$$

For $\Omega_{GW} \approx 9.3_{-4.0}^{+5.8} \times 10^{-9}$ [1, 2] we have the critical density of GWs as follows $\Omega_{GW*} \sim 10^{-29} - 10^{-30}$. The number of e-folds can be given by [39, 40]:

$$N = \frac{1}{\epsilon_H} \int_H^{H_{end}} d \ln H' = \frac{1}{\epsilon_H} \ln \frac{H_{end}}{H}. \quad (3.9)$$

Here, $\epsilon_H = -\frac{\dot{H}}{H^2} \ll 1$ is the slow roll parameter. This relationship corresponds with observations data, because if we take $H = H_{end}$ we find the value of N at the end of inflation ($N = 0$). We can additionally calculate the H concerning f using the following approach:

$$H(f) = H_{end} \left(\frac{f}{f_*} \right)^{\epsilon_H}. \quad (3.10)$$

In the scenario where $f_* = f$, we arrive at $H(f) = H_{end}$. Conversely, in the case of (3.6), we achieve

$$H(f) < H_{end}. \quad (3.11)$$

We recall that the assessment of the present rate of the Universe's expansion yields $H_0 \simeq (73.24 \pm 1.74) km.s^{-1}.Mpc^{-1}$ [20]. Conversely, measurements of the Hubble constant based on the CMB result is $H_0 \simeq (67.27 \pm 0.66) km.s^{-1}.Mpc^{-1}$ [21]. The Hubble tension's behavior reveals a diminishing value of H as time elapses. This shows that according to (3.11) the Hubble parameter $H(f)$ characterizes the inflationary epoch. This is underscored by the fact that H_{end} signifies the end of inflation. Consequently, the frequencies f detected by the NANOGrav collaboration are indicative of the inflationary era.

4 Inflationary scenario from e-folding number

Thereafter we want to seek the relationship between the current amplitude of the gravitational wave signal and frequency. We recall that $\dot{N} = -H$ [41], i.e. $\dot{N} = -\frac{\dot{f}}{f}$ (3.5). Consequently, this leads to

$$H = \frac{\dot{f}}{f}. \quad (4.1)$$

This result implies that the Hubble parameter represents the logarithmic variation of GW frequency. If we compare (4.1) with the definition of the Hubble parameter $H = \frac{\dot{a}}{a}$, we find $f = af_0$ with f_0 is a constant with frequency unit. This proportionality between the scale factor and frequency can establish a link between the Hubble tension problem and the NANOGrav 15-yr result. The slow roll parameter $\epsilon_H = -\frac{\dot{H}}{H^2}$ can be written as

$$\epsilon_H = 1 - \frac{\ddot{f}f}{\dot{f}^2}. \quad (4.2)$$

Introducing these parameters

$$\sigma = \frac{\ddot{f}}{\dot{f}^2}, \quad \lambda = \frac{\ddot{\dot{f}}}{\dot{f}} \frac{1}{\dot{f}}. \quad (4.3)$$

From this model, the slow-roll parameter $\eta = \epsilon_H - \frac{\dot{\epsilon}_H}{2H\epsilon_H}$ [41] is given by

$$\eta = 1 - \sigma f - \frac{f}{2(1 - \sigma f)} (2\sigma^2 f - \lambda\sigma f - \sigma). \quad (4.4)$$

In the inflationary scenario, the ϵ_H grows as well $d\epsilon_H/dN = 2\epsilon_H(\eta - \epsilon_H)$. The spectral index of perturbations is equal to [41]:

$$n_s = 1 - 6\epsilon_H + 2\eta. \quad (4.5)$$

Thus, the spectral index (see Appendix A) can be written as

$$n_s = -3 + 4\sigma f - \frac{f}{1 - \sigma f} (2\sigma^2 f - \lambda\sigma f - \sigma). \quad (4.6)$$

If $\lambda = 2\sigma$, we can estimate the spectral index by the ratio $n_s \approx -3 + 4\sigma f + \frac{\sigma f}{1 - \sigma f}$. If $f = 0$ we obtain $n_s = -3$. From (3.7) and (4.6) we get

$$\Omega_{GW}(f) = \Omega_{GW*} \exp N(-3 + 4\sigma f - \frac{\sigma f}{1 - \sigma f} (2\sigma f - \lambda f - 1)), \quad (4.7)$$

where Ω_{GW*} is the amplitude at the typical frequency f_* . The amplitude at $f = 0$ is given by $\Omega_{GW}(f) = \Omega_{GW*} e^{-6N}$.

5 Stochastic GW signals at preheating

Thereafter, we want to study the spectral index from the relationship (3.10) instead of (4.1): $H(f) = H_{end} \left(\frac{f}{f_*}\right)^{\epsilon_H}$. We calculate the derivative of this parameter with respect to time (see Appendix A), and we determine

$$\frac{\dot{H}(f)}{H(f)} = \dot{\epsilon}_H \ln\left(\frac{f}{f_*}\right) + \epsilon_H \frac{\dot{f}}{f}. \quad (5.1)$$

Using $\epsilon_H = -\frac{\dot{H}}{H^2}$, we can relate the slow roll parameter ϵ_H to GW frequency as

$$-\frac{H\epsilon_H}{\dot{\epsilon}_H} = \ln\left(\frac{f}{f_*}\right) + \frac{\epsilon_H \dot{f}}{\dot{\epsilon}_H f}, \quad (5.2)$$

and hence it can be written as

$$\epsilon_H - \frac{\dot{\epsilon}_H}{2H\epsilon_H} = \epsilon_H + \frac{1}{2} \left[\ln\left(\frac{f}{f_*}\right) + \frac{\epsilon_H \dot{f}}{\dot{\epsilon}_H f} \right]^{-1}. \quad (5.3)$$

Therefore, the slow-roll parameter $\eta = \epsilon_H - \frac{\dot{\epsilon}_H}{2H\epsilon_H}$ [41] is given by $\eta = \epsilon_H + \frac{1}{2} \left[\frac{\epsilon_H \dot{f}}{\dot{\epsilon}_H f} + \ln\left(\frac{f}{f_*}\right) \right]^{-1}$.

Thus, the spectral index $n_s = 1 - 6\epsilon_H + 2\eta$ can be written as

$$n_s = 1 - 4\epsilon_H + \left[\frac{\epsilon_H \dot{f}}{\dot{\epsilon}_H f} + \ln\left(\frac{f}{f_*}\right) \right]^{-1}. \quad (5.4)$$

If $\sigma f = 1$, one obtain $n_s = 1 + \ln^{-1}\left(\frac{f}{f_*}\right)$, i.e. $\Omega_{GW}(f) = \Omega_{GW*} e^{(1+\ln^{-1}(\frac{f}{f_*}))N}$. Next, we consider $\sigma = \frac{\dot{f}}{f^2}$ to be a constant and we obtain $\epsilon_H = 1 - \sigma f$, this yields $\frac{\dot{\epsilon}_H}{\epsilon_H} = \frac{-\sigma \dot{f}}{1 - \sigma f}$. The n_s with respect to f is given by

$$n_s = -3 + 4\sigma f + \left[-\frac{1 - \sigma f}{\sigma f} + \ln\left(\frac{f}{f_*}\right) \right]^{-1}, \quad (5.5)$$

and the energy density spectrum can be written as

$$\Omega_{GW}(f) = \Omega_{GW*} \exp N \left(-3 + 4\sigma f + \left[-\frac{1 - \sigma f}{\sigma f} + \ln\left(\frac{f}{f_*}\right) \right]^{-1} \right). \quad (5.6)$$

In Figure (1) we plot the n_s as a function of the frequency f . In this illustration, it's evident that the curves representing the function $n_s(f)$ intersect with the range of observed values. While, in Figures (2)-(3) we plot the energy density spectrum $\Omega_{GW} h^2$ as it varies with frequency f .

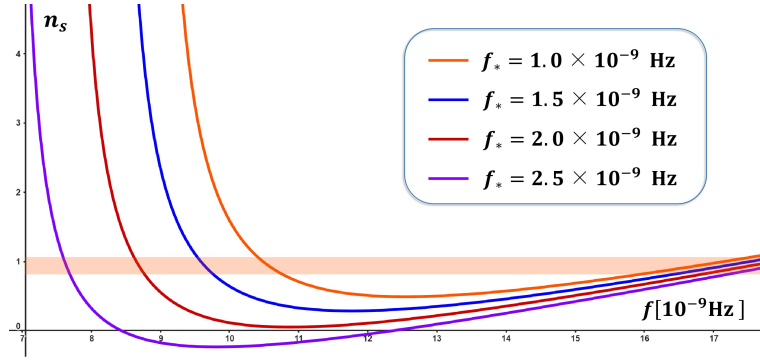


Figure 1: Evolution of model parameters n_s (5.5) for $\sigma = 5 \times 10^7$ and $nHz \leq f_* \leq 2.5nHz$.

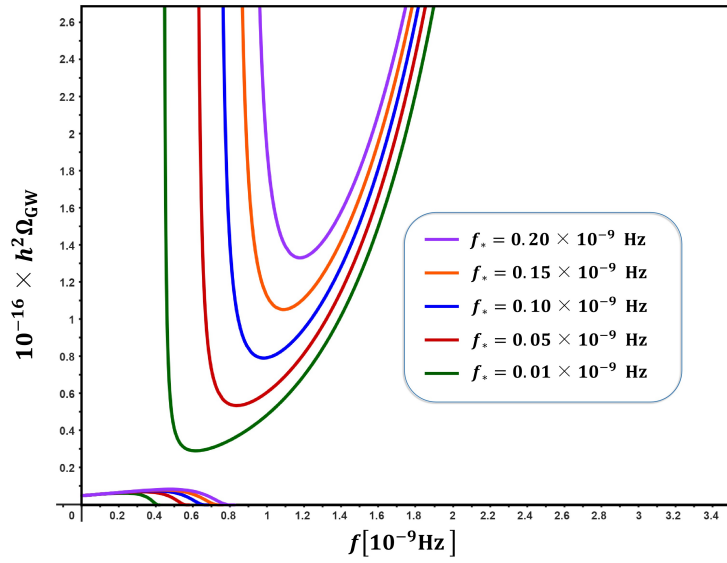


Figure 2: Evolution of energy density spectrum $\Omega_{GW}h^2$ (5.6) for $\sigma = 5 \times 10^7$ and $N = 1$ with $nHz \leq f_* \leq 2.5nHz$.

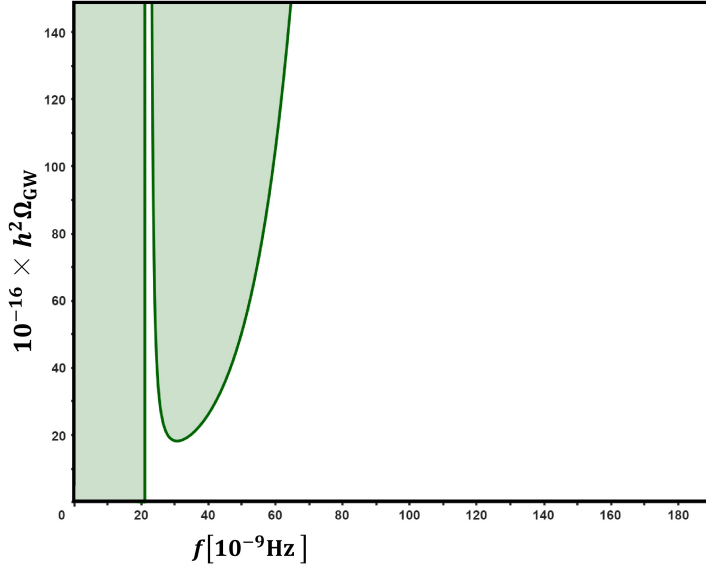


Figure 3: Region of the gravitational wave spectrum for $\sigma = 10^7$, $\Omega_{GW*} \sim 10^{-14}$, $N = 2$ and $f_* = 0.5nHz$.

In Figure (3), we observe two distinct regions delineating the GW frequency characteristics of the early universe. The interval $0nHz \leq f \leq 20nHz$ corresponds to the outcomes associated with the CMB. Notably, the interval $f \sim 25nHz - 65nHz$ characterizes the dataset generated by the NANOGrav 15-yr result at the (near) end of inflation $N \sim 2$. These results directly match the observed data [1, 2, 36]. This constraint on f has significant implications for the energy density spectrum of gravitational waves, $\Omega_{GW}h^2$, at PTA frequencies. A vanishing GW frequency, which would imply a nearly scale-invariant GW spectrum, corresponds to the first instance of the universe. The study suggests that there exists an intermediate range of frequencies between those of CMB and PTA, which lacks energy density spectrum. components.

We consider that $\sigma f \ll 1$ and $-3 + 4\sigma f - \frac{\sigma f}{1-\sigma f} = 0$, thus, (5.5) can be written as $n_s \approx -\left(\frac{\sigma f}{1-\sigma f}\right)^2 \ln\left(\frac{f}{f_*}\right)$. The energy density spectrum is estimated as

$$\Omega_{GW}(f)h^2 = \Omega_{GW*}h^2 \left(\frac{f}{f_*}\right)^{-\left(\frac{\sigma f}{1-\sigma f}\right)^2 N}. \quad (5.7)$$

If we use $k = 2\pi f$ with $k_* = 2\pi f_*$ is the characteristic scale, we find that $\Omega_{GW}(f) = \Omega_{GW*} \exp\left(-\ln\left(\frac{k}{k_*}\right) \left(\frac{\sigma f}{1-\sigma f}\right)^2 N\right)$, which exactly corresponds to the primordial power spectrum of curvature perturbations $\mathcal{P}_{\mathcal{R}}(f)$ [37, 38], also it checked equation (3.1). The relation (5.7) is in good agreement with (2.6) and the NANOGrav's observations, suggesting that $\Omega_{GW} \propto f^\zeta$ with $\zeta \in (-1.5, 0.5)$ at a frequency of $f = 5.5nHz$. Combining

this with (5.7) we get

$$\zeta = - \left(\frac{\sigma f}{1 - \sigma f} \right)^2 N < 0. \quad (5.8)$$

In the scenario where $\sigma \sim 10^7$, as illustrated in Figures (2)-(3), we determine that $\zeta = -0.143876N < 0$. This conclusion subsequently implies the following condition: $0 \leq N \leq 10.425$. Furthermore, this range ensures that ζ remains greater than or equal to -1.5 . In the tables below (1), we analyze numerical representations of the relationship (5.8).

N	ζ	$\sigma [s]$
60	-1.5	2.482×10^7
60	-0.5	1.520×10^7
60	-10^{-6}	2.346×10^4
50	-1.5	2.684×10^7
50	-0.5	1.652×10^7
2	-0.5	6.060×10^7

Table 1: The stochastic gravitational wave background based on the value of the Hubble constant for $f = 5.5nHz$.

Based on these results, it is worth noting that the values of ζ precisely satisfy the data conditions indicating that the relationship (3.10) aligns well with the observational data. The range $0 \leq N \leq 10.425$ signifies the epoch marking the end of inflation. During this period, there is the emission of stochastic gravitational waves, which are then detected by the NANOGrav collaboration. From the relationship (5.8) we deduce $N(f) = \left(\frac{1-\sigma f}{\sigma f} \right)^2 |\zeta|$ and $f = \frac{1}{\sigma(1+\sqrt{\frac{N}{|\zeta|}})}$. From this, we plot the curve of N as a function of f in figure (4).

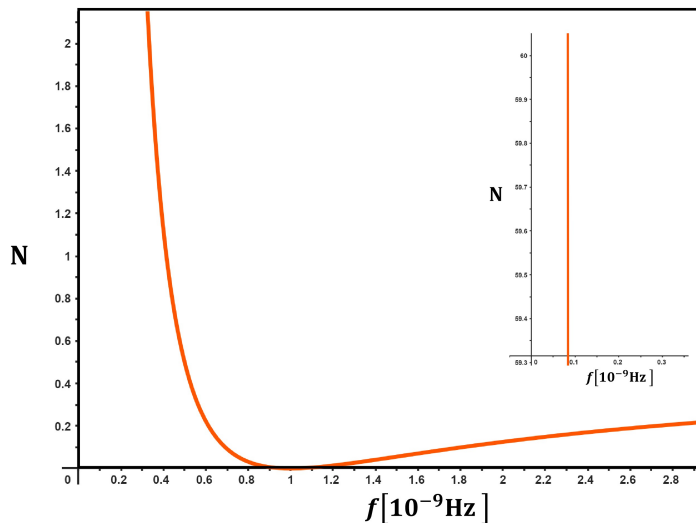


Figure 4: N curve as a function of f , such as $\sigma = 1.5 \times 10^7 s$ and $\zeta = -0.5$.

In Figure (4), we observe that when considering the CMB with $30 \leq N \leq 60$ [42], the frequency of the GW signal f remains consistently close to the value $f = 0.08nHz$. However, as we approach the end of inflation, the range of $N \leq 1$ values encompasses two distinct frequency values. Finally, at the precise end of inflation ($N = 0$), the frequency settles at a singular value, which is equal to $f = 1nHz$. The sharp increase in frequency observed towards the end of the inflationary period indicates a significant cosmic variation. This change is due to the curvature perturbation [19].

The state of the universe at the the end of inflation is known as the preheating [18]. Typically, following the end of inflation, our Universe will transition into a radiation-dominated era, during which perturbations will once again enter the observable horizon.

6 Conclusion

In summary, the study has explored the stochastic gravitational wave produced during the end of inflation. In this context, it has been established that the Hubble parameter is linked to the logarithmic variation of GW frequency. By analyzing the frequencies detected by the NANOGrav collaboration in relation to the end of inflation marked by H_{end} , we have unveiled a significant connection. This connection suggests a logarithmic relationship between the Hubble parameter and gravitational wave frequency, represented as $f \propto a$, where a represents the scale factor. This proportional link between scale factor and frequency could shed light on the Hubble tension problem and its connection to the NANOGrav 15-yr results. Furthermore, we present plots of the spectral index n_s as a function of frequency f , showing how $n_s(f)$ intersects with observed values.

We have also explored the energy density spectrum $\Omega_{GW}h^2$ in relation to frequency, revealing two distinct regions in Figure (3), corresponding to GW frequencies associated with the early universe and those generated by NANOGrav 15-yr results at the end of inflation. These results align with observed data, emphasizing the importance of frequency constraints for the energy density spectrum of gravitational waves at PTA frequencies. Notably, an absence of energy density spectrum components is identified in an intermediate frequency range, bridging the CMB and PTA domains. In Figure (4), we have observed the behavior of GW signal frequency concerning the CMB for different inflationary parameters. Remarkably, as we approach the end of inflation ($N \leq 1$), two distinct frequency values emerge. At the precise end of inflation ($N = 0$), the frequency stabilizes at a singular value, $f = 1nHz$. This study proposes that primordial universe scenarios, which rely on the emission of the stochastic gravitational waves at the end of inflation, can offer a new period of the emission of this stochastic gravitational wave background. This could result in a greater likelihood of observing distinct signals in PTA observations.

7 Appendix A

1- Inflationary scenario from e-folding number

From $\dot{N} = -H$ we have $\dot{N} = -\frac{\dot{f}}{f} = -H$, which leads to $H = \frac{\dot{f}}{f}$. From this we get

$$\dot{H} = \frac{\ddot{f}f - \dot{f}^2}{f^2}. \quad (7.1)$$

We employ the constraint $\epsilon_H = -\frac{\dot{H}}{H^2} = \frac{\dot{f}^2 - \ddot{f}f}{\dot{f}^2}$ derived from $\epsilon_H = -\frac{\dot{H}}{H^2}$ and we find

$$\epsilon_H = 1 - \frac{\ddot{f}f}{\dot{f}^2} = 1 - \sigma f, \quad (7.2)$$

where $\sigma = \frac{\ddot{f}}{\dot{f}^2}$ and $\lambda = \frac{\ddot{f}}{f} \frac{1}{\dot{f}}$. Using $2H\epsilon_H = 2\frac{\dot{f}^2 - \ddot{f}f}{\dot{f}f}$ and $\frac{1}{2H\epsilon_H} = \frac{f}{2(\dot{f}^2 - \ddot{f}f)}$ we can calculate the slow-roll parameter $\eta = \epsilon_H - \frac{\dot{\epsilon}_H}{2H\epsilon_H}$. We have

$$\dot{\epsilon}_H = 2 \left(\frac{\ddot{f}}{\dot{f}} \right)^2 \frac{f}{\dot{f}} - \frac{\ddot{f}}{\dot{f}^2} f - \frac{\ddot{f}}{\dot{f}}, \quad (7.3)$$

which leads to

$$\eta = 1 - \frac{\ddot{f}f}{\dot{f}^2} - \frac{f}{2 \left(1 - \frac{\ddot{f}f}{\dot{f}^2} \right)} \left(2 \left(\frac{\ddot{f}}{\dot{f}} \right)^2 \frac{f}{\dot{f}^2} - \frac{\ddot{f}}{\dot{f}} \frac{f}{\dot{f}^2} - \frac{\ddot{f}}{\dot{f}^2} \right). \quad (7.4)$$

So we can relate the slow-roll parameter to frequency of the GW signal f as

$$\eta = 1 - \sigma f - \frac{f}{2(1 - \sigma f)} (2\sigma^2 f - \lambda \sigma f - \sigma). \quad (7.5)$$

We can additionally calculate the spectral index using the following approach: the spectral index $n_s = 1 - 6\epsilon_H + 2\eta$ is

$$n_s = 1 - 6 + 6\sigma f + 2 - 2\sigma f - \frac{f}{(1 - \sigma f)} (2\sigma^2 f - \lambda\sigma f - \sigma). \quad (7.6)$$

So, we find equation (4.5):

$$n_s = -3 + 4\sigma f - \frac{f}{(1 - \sigma f)} (2\sigma^2 f - \lambda\sigma f - \sigma). \quad (7.7)$$

2- Inflationary scenario from Hubble parameter

From the relationship (3.10) $H(f) = H_{end} \left(\frac{f}{f_*}\right)^{\epsilon_H}$ we have

$$\dot{H}(f) = \frac{d}{dt} \left(\epsilon_H \ln \left(\frac{f}{f_*} \right) \right) H(f), \quad (7.8)$$

where

$$\frac{d}{dt} \left(\epsilon_H \ln \left(\frac{f}{f_*} \right) \right) = \dot{\epsilon}_H \ln \left(\frac{f}{f_*} \right) + \epsilon_H \frac{\dot{f}}{f},$$

which leads to

$$\frac{\dot{H}(f)}{H(f)} = \left(\dot{\epsilon}_H \ln \left(\frac{f}{f_*} \right) + \epsilon_H \frac{\dot{f}}{f} \right). \quad (7.9)$$

Using $\epsilon_H = -\frac{\dot{H}}{H^2}$, so we find equation (5.1) $-H\epsilon_H = \dot{\epsilon}_H \ln \left(\frac{f}{f_*} \right) + \epsilon_H \frac{\dot{f}}{f}$.

References

- [1] Afzal, A., et al. and NANOGrav Collaboration, 2023, The Astrophysical Journal Letters, 951(1), L11.
- [2] G. Agazie et al. and NANOGrav Collaboration, 2023, The Astrophysical Journal Letters, 951(1), L8.
- [3] Arzoumanian, Z., et al. and NANOGrav Collaboration, 2020, The Astrophysical Journal Letters, 905(2), L34.
- [4] Arzoumanian, Z., et al. and NANOGrav Collaboration, 2021, Physical review letters, 127(25), 251302.
- [5] Antoniadis, J., et al., 2022, Monthly Notices of the Royal Astronomical Society, 510(4), 4873-4887.
- [6] Middleton, H., et al., 2021, Monthly Notices of the Royal Astronomical Society: Letters, 502(1), L99-L103.

- [7] Zhang, Z., Cai, C., Su, Y. H., Wang, S., Yu, Z. H., and Zhang, H. H., 2023, arXiv preprint arXiv:2307.11495.
- [8] Vagnozzi, S., 2023, *Journal of High Energy Astrophysics*, 39, 81-98.
- [9] An, H., Su, B., Tai, H., Wang, L. T., and Yang, C., 2023, arXiv preprint arXiv:2308.00070.
- [10] Niu, X., and Rahat, M. H., 2023, arXiv preprint arXiv:2307.01192.
- [11] Mansoori, S. A. H., Felegray, F., Talebian, A., and Sami, M., 2023, *Journal of Cosmology and Astroparticle Physics*, 2023(08), 067.
- [12] Cheung, K., Ouseph, C. J., and Tseng, P. Y., 2023, arXiv preprint arXiv:2307.08046.
- [13] Bousder, M., Riadsolh, A., Fatimy, A. E., Belkacemi, M. E., and Ez-Zahraouy, H., 2023, arXiv preprint arXiv:2307.10940.
- [14] Bousder, M. (2022). A new constant behind the rotational velocity of galaxies. *Journal of Cosmology and Astroparticle Physics*, 2022(01), 015.
- [15] Bousder, M., Salmani, E., & Ez-Zahraouy, H. (2023). Entropy as logarithmic term of the central charge and modified Friedmann equation in AdS/CFT correspondence. *Journal of High Energy Astrophysics*, 38, 49-57.
- [16] Bousder, M., & Bennai, M. (2021). Particle-antiparticle in 4D charged Einstein-Gauss-Bonnet black hole. *Physics Letters B*, 817, 136343.
- [17] Ellis, J., Lewicki, M., Lin, C., and Vaskonen, V., 2023, arXiv preprint arXiv:2306.17147.
- [18] Easter, R., Giblin Jr, J. T., and Lim, E. A., 2007, *Physical Review Letters*, 99(22), 221301.
- [19] Lyth, D. H., 2005, *Journal of Cosmology and Astroparticle Physics*, 2005(11), 006.
- [20] Riess, A. G., et al., 2016, *The Astrophysical Journal*, 826(1), 56.
- [21] Aghanim, N., et al., 2020, *Astronomy & Astrophysics*, 641, A6.
- [22] Di Valentino, et al., 2021, *Classical and Quantum Gravity*, 38(15), 153001.
- [23] Vagnozzi, S., 2023, *Universe*, 9(9), 393.
- [24] Schiavone, T., Montani, G., and Bombacigno, F., 2023, *Monthly Notices of the Royal Astronomical Society: Letters*, 522(1), L72-L77.

- [25] Yang, Y., Lu, X., Qian, L., & Cao, S., 2023, Monthly Notices of the Royal Astronomical Society, 519(4), 4938-4950.
- [26] Monjo, R., & Campoamor-Stursberg, R., 2023, Classical and Quantum Gravity.
- [27] Poulin, V., Smith, T. L., Karwal, T., and Kamionkowski, M., 2019, Physical review letters, 122(22), 221301.
- [28] Jedamzik, K., and Pogosian, L., 2020, Physical Review Letters, 125(18), 181302.
- [29] Christensen, N., 2018, Reports on Progress in Physics, 82(1), 016903..
- [30] Kuroyanagi, S., Chiba, T., and Takahashi, T., 2018, Journal of Cosmology and Astroparticle Physics, 2018(11), 038..
- [31] Zhao, W., Zhang, Y., You, X. P., and Zhu, Z. H., 2013, Physical Review D, 87(12), 124012.
- [32] Liu, X. J., Zhao, W., Zhang, Y., and Zhu, Z. H., 2016, Physical Review D, 93(2), 024031.
- [33] Vagnozzi, S., 2021, Monthly Notices of the Royal Astronomical Society: Letters, 502(1), L11-L15.
- [34] Bian, L., Ge, S., Li, C., Shu, J., and Zong, J., 2022, arXiv preprint arXiv:2212.07871.
- [35] Domcke, V., Pieroni, M., and Binétruy, P., 2016, Journal of Cosmology and Astroparticle Physics, 2016(06), 031.
- [36] Niu, X., & Rahat, M. H., 2023, arXiv preprint arXiv:2307.01192.
- [37] Liu, L., Chen, Z. C., and Huang, Q. G., 2023, arXiv preprint arXiv:2307.14911.
- [38] Chang, Z., Kuang, Y. T., Wu, D., and Zhou, J. Z., 2023, arXiv preprint arXiv:2309.06676.
- [39] Bousder, M., Riadsolh, A., El Belkacemi, M. and Ez-Zahraouy, H., 2023, Annals of Physics, 458, 169441.
- [40] Bousder, M., Salmani, E., El Fatimy, A., & Ez-Zahraouy, H., 2023, Annals of Physics, 452, 169282.
- [41] Maartens, R., Wands, D., Bassett, B. A., and Heard, I. P., 2000, Physical Review D, 62(4), 041301.
- [42] Giarè, W., Forconi, M., Di Valentino, E., & Melchiorri, A., 2023, Monthly Notices of the Royal Astronomical Society, 520(2), 1757-1773.